ISSN 2079-0961, Arid Ecosystems, 2020, Vol. 10, No. 1, pp. 10–16. © Pleiades Publishing, Ltd., 2020.
Russian Text © The Author(s), 2020, published in Aridnye Ekosistemy, 2020, Vol. 26, No. 1(82), pp. 13–20.

SYSTEMATIC STUDY OF ARID TERRITORIES

Landscape Approach to the Modeling of Land-Cover Dynamics with Remote Methods

T. I. Kharitonova[a], * and N. V. Surkov[a]

[a]*Moscow State University, Department of Geography, Moscow, 119991 Russia*

**e-mail: kharito2010@gmail.com*

Received May 10, 2019; revised August 29, 2019; accepted September 30, 2019

Abstract—The article discusses remote methods for the description of the intraseasonal dynamics of soil and vegetation moisture. The field moisture content of the soil and vegetation cover is described by an integral indicator that takes into account the moisture content of the upper soil horizon (5–10 cm), grass phytomass, and leaves of trees and shrubs. The integrated field moisture demonstrates a reliable association with the normalized differential water index (NDWI); the determination coefficient R^2 reaches values of 0.91 for individual classes of tracts. The most significant factors determining the loss of moisture during the summer period are the amount of photosynthetically active phytomass, the potential influx of solar radiation during the study period, and the moisture reserve in the soil and vegetation at the beginning of the growing season. These factors describe 67% of the NDWI difference between May and August 2016 in forest areas and 89% in the steppes. The results can be used to search for fire hazardous areas in the steppes and forests, as well as for the monitoring of vineyards.

Keywords: Karadag Nature Reserve, land-cover moisture, NDWI, semiarid landscapes of Crimea

DOI: 10.1134/S2079096120010096

INTRODUCTION

Monitoring the moisture content of the land cover (LC) is primarily important to predict the biological production of ecosystems, to calculate irrigation rates in agriculture, and to ensure timely fire-fighting measures. Three approaches to the remote determination of moisture have been developed: one approach based on reflection by the Earth's surface of solar radiation in the visible and infrared ranges of wavelengths (0.4–2.5 μm) and approaches based on the reflection and intrinsic radiation of the Earth's surface in the thermal (10–13 microns) and microwave (2.7 mm–30 cm) ranges.

The recognition of microwave data is based on the close relationship between the dielectric constant of the soil and its moisture: with increasing moisture, the dielectric constant increases and the microwave flux increases (Dobson and Ulaby, 1985). At the same time, the microwave signal depends on the topography, surface roughness, and the properties of the vegetation cover. Since soil moisture is studied mainly in dynamics, the characteristics of the relief and surface roughness are assumed to be unchanged for the studied period. With all of the above assumptions, soil moisture models based on active and passive microwave receivers show relatively high accuracy with R^2 from 0.49 to 0.67 (Escorihuela, Quintana-Seguí, 2016). Models built for flat surfaces with more or less uniform vegetation, i.e., for agricultural fields show higher reliability (R^2 up to 0.85) (Wigneron et al., 1995).

The main advantage of remote sensing systems operating in the microwave range is broadband imaging, which allows daily or even twice-daily reception of data on the state of the Earth's surface (AMSR-E, AMSR2). A significant drawback is their small scale: for AMSR receivers, the spatial scale is 5.4–56 km depending on the wavelength. At the SMAP receiver, the resolution is increased to 1–3 km with a reduction of the shooting frequency to 2–3 days.

The interpretation of the thermal data is based on the dependence of the difference in air temperature and the Earth's surface on the evaporation intensity (Seneviratne et al., 2010). An increase in temperature difference signals a slowdown in evaporation and, accordingly, a lack of water in the soil. This technique gives a fairly accurate result for the calculation of irrigation rates in fields with more or less similar crops (Ghulam et al., 2008). The heterogeneity of vegetation creates modeling errors in studies of a more complex landscape cover. The surface temperature of the soil and leaves is calculated based on the data of thermal satellite imagery, while the air temperature must be obtained instrumentally, which creates additional complexity for this approach.

The more common method suggested by M.S. Moran et al. (1994), is a statistical simulation of

soil moisture deficiency in the factor space of the brightness of the Earth's surface and the normalized difference vegetation index (NDVI). The essence of the method lies in the fact that each phytocenosis has lower and upper boundaries of the brightness temperature, which correspond to the states of complete saturation of soil moisture and its complete desiccation. The temperature of the bare soil varies over wider ranges. All combinations of temperature and NDVI form a trapezoid figure in the attribute space. The trapezoid shape is regionally specific and requires a large amount of field material collected in different landscape and climatic conditions for accurate determination (Carlson, 2007). With a good model calibration, the reliability of the determination of the moisture deficit is high: $R^2 = 0.6–0.9$ (Sadeghi et al., 2017). Satellite imagery performed simultaneously in the optical and thermal ranges allows information about the state of the Earth's surface to be obtained fairly quickly.

The study of the moisture of the Earth's surface according to optical data is based on the change in the reflectance of the sheet in the near and middle infrared ranges (NIR 700–1300 nm, NIR 1300–3000 nm), which is determined by the change in the cellular structure of the sheet during dehydration (Peuelas et al., 1993) and directly depends on the actual water content in sheet (Gillon et al., 2004; Yebra et al., 2013). The method of estimating the moisture content in the vegetation cover from remote data is justified in the works of B.-C. Gao (1996) and P. Ceccato et al. (2002). All methods are based on the ratio of reflection in the near and middle infrared ranges, which is expressed in different versions of the spectral moisture indices with various corrections.

The above methods have the same features. First, all of them are based on the axiom of the close dependence of soil moisture and vegetation. It is assumed that the reflection of ungraded soil provides information about the moisture content of the upper 5–10 cm of soil, and vegetation provides information about the moisture content of the root layer. All methods tend to result in data on either the soil moisture (which is used in the interpretation of microwave and thermal radiation), in which case the vegetation is noise, (Shvetsov et al., 2013), or on the phytomass moisture (in the case of interpretation of optical channels), in which case large errors are observed in areas with sparse vegetation. Second, all models are calibrated not for the absolute values of the moisture content in the soil and vegetation but for its deviation from the minimum or maximum content, most often for a moisture deficit. Third, the process of moisture loss proceeds differently in different environmental conditions. Models are most often calibrated for different types of vegetation cover (Ceccato et al., 2002), but there are already works that take into account landscape heterogeneity, so W. Nijland et al. (2015) used the edaphic matrix of Pogrebnyak to study moisture reserves in the forest crown. Fourth, all models give high confidence indicators in relatively flat areas; their use in mountainous areas is either impossible (microwave imaging) or is poorly studied.

The goal of this study was to construct a statistical model to estimate the seasonal dynamics of moisture in the soil and vegetation cover of the landscapes of the eastern tip of the Crimean Mountains according to the Landsat-8 optical survey. The contributions of soil moisture, grass moisture, shrub, and wood tiers to the integral reflection were differentiated via the introduction of an indicator that takes into account the share of each tier in the overall signal. The progressive desiccation of the territory during the summer period (Transformation ..., 2009) made it possible to evaluate the dynamics of moisture of the soil and vegetation cover in relation to the most humid conditions observed in mid-May. Modeling was carried out for classes of tracts reflecting the diversity of vegetation, exposure, and morphometry of the relief.

MATERIALS AND METHODS

Thirty-eight points of landscape descriptions and sampling were laid in the territory of the Karadag reserve and the Echkidag reserve (Fig. 1). Samples of wood foliage (if any) and mowings from grass vegetation on an area of 50 × 50 cm with significant projective cover were taken. Samples of litter and dry weight of cereals or moss cover were separately taken. Soil samples were taken by the envelope method from a depth of 5–10 cm. Sampling from the top 5 cm was not performed, because the intraday fluctuations in moisture in them are more pronounced and its dynamics is "lost" over longer time periods (Gorbunov et al., 2015). The moisture content of the samples was determined by the gravimetric method and was calculated as the ratio of the mass loss during drying to the mass of the wet sample.

Morphometric analysis of the relief was carried out on the basis of a digital elevation model with a spatial resolution of 30 m. It was constructed via ordinary kriging along horizontal lines digitized from a topographic base of scale 1 : 50000. The potential redistribution of moisture along the relief was estimated by the SAGA Wetness Index and calculated as the logarithm of a relationship specific catchment area to the slope of this raster cell (Böhner, Selige, 2006). The potential solar radiation was calculated in the SAGA program based on the morphometry of the relief, the height of the sun, and the duration of daylight hours (Sysuev, 2003).

The actual soil moisture, which is defined as the hypothetical thickness of the water layer in a plant leaf or the thin surface layer of the substrate, was estimated with the normalized differential moisture index (NDWI) with the formula NDWI = (NIR-SWIR)/(NIR + SWIR), where NIR is reflection in the near-infrared range and

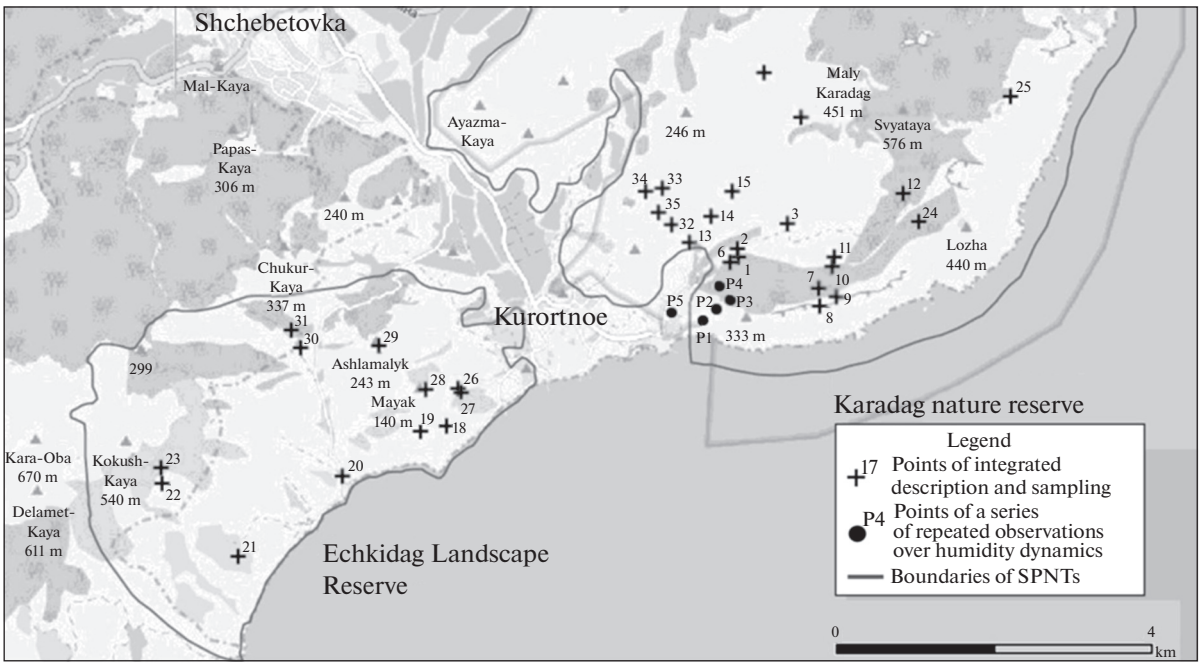

Fig. 1. Study area and sampling points.

SWIR is the reflection in the mid-infrared wavelength range (Maki et al., 2004). Cloudless Landsat-8 images were used for May 14, June 15, and August 27, 2016. The NDVI was calculated for the same images.

Since the brightness value of a pixel is formed due to reflection from the entire surface at its borders, it may turn out to be partly the crown of a tree or bush, a layer of grass vegetation, or bare soil. In this work, the moisture of the soil and vegetation cover is described by an integral indicator that combines the values of soil moisture, grass phytomass, and tree foliage. Thus, we obtain a field layer of water in the soil-vegetation cover visible for satellite imagery. It is calculated as:

$$B = aB_{\text{leaf}} + bB_{\text{herb}} + cB_{\text{soil}},$$

where B is the integral humidity, B_{herbs} is the humidity of the herbal phytomass, B_{soils} is the humidity of the upper soil layer, B_{sheet} is the humidity of the foliage, and a is the closeness of the tree crowns; b is the projective cover of the grass layer in fractions of unity when $(a + b) \le 1$ and is taken as equal to $(1 - a)$ when there is a partial overlap of the tiers; c is the fraction of exposed soil calculated as $1 - (a + b)$ and is taken as equal to zero for $(a + b) > 1$. The sum of the coefficients a, b, and c is equal to 1, and they are taken into account in the order of tiering.

Analysis of the dynamics of humidity was carried out with allowance for the landscape conditions of the territory. The controlled classification of Landsat-8 multizone images was applied to construct a map of the classes of tracts with a method to extract the three main components. Within each class of landscape cover, a division was made according to the relief. The relief is described by two parameters: steepness and slope exposure. In this work, three classes of steepness (surfaces with an inclination of up to 10°, 10–25° and more than 25°) and two exposure classes (cold and warm, with azimuths between 125° and 305° as the boundary between them) are distinguished. A total of 17 classes of natural complexes were obtained, of which 14 were characterized by a network of observations (Fig. 2).

RESULTS AND DISCUSSION

Landscape Structure of the Territory. The study area is characterized by high landscape diversity due to the difference in absolute heights, the geological foundation, and the slope exposure. The upper floors of the mountains are occupied by rocky oak forests with hawthorn, ash, and dogwood on brown forest soils and fluffy oak forests with pistachio, ash, and juniper on brown soils. Petrophytic steppes with sparse and low grass stand alternating with exposed soil form on outcrops of dense limestone and volcanic rocks above 200 m. Pistachio–oak woodlands with a tree stand are widespread on the deluvial-colluvial plumes and the lower parts of the slopes, which are composed of Neogene-Quaternary loose rocks. On the southern slopes and flat sea terraces, they are replaced by steppes: from dry Aegilops fescue to more humid feather grass and grasses. In some areas of the terraced slopes there are pine plantings. North of the village, the resort has vineyards. In total, forest LC accounts for 21.2% of the area, sparse forests constitute 31.9%, steppe forests occupy 29.1%, outcrops of rock and loose species

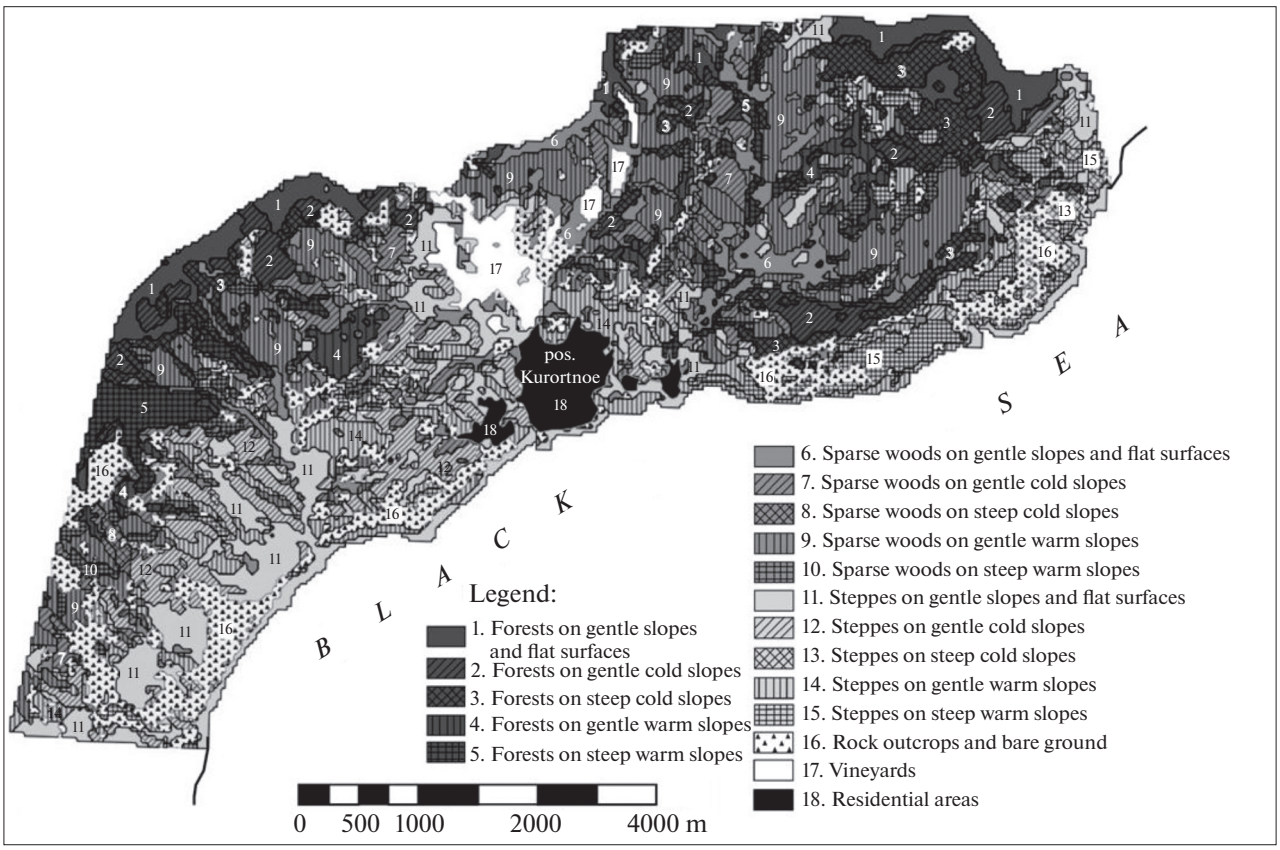

Fig. 2. Tract classes.

account for 12.5%, and residential lands and vineyards occupy 2.6 and 2.7% of the area, respectively.

Field Moisture of the LC. The landscape diversity determines the high variability of soil moisture and vegetation. The highest soil moisture (34%) was recorded in trunk bottoms covered with sparse wood from ash and wood, in oak–ash forests with developed grass and moss cover, and on the sloping northern slopes, composed of loose rocks. The points with the driest soil (13%) are confined to steep southern and southwestern slopes with sparse, fluffy oak forests or with petrophytic steppes. Dry soils are also characteristic of the middle parts of slopes or colluvial loops with stony soils, which can quickly carry moisture down from the upper horizons. Natural complexes exposed to cattle grazing or unorganized recreation are characterized by lower values of soil moisture (up to 10–12%) than their analogs in the conservation area.

The moisture reserve in the leaves of the tree–shrub layer primarily depends on the species composition. There is less moisture in the foliage of fluffy oak (44–47%) and a dense undergrowth from the hawthorn, which is more typical for the shaded slopes of the northern exposure. The average humidity of the foliage of such forests reaches 68–71%. The maximum moisture content of grassy phytomass was recorded under the dense canopy of forest–oak forests and pine plantations (75–80%). Communities of meadow steppes also have a high supply of moisture (67–73%). The lowest moisture content of the grass layer was recorded in the steppe LC of terraces and colluvial plumes and in the forest LC of flat, expanded trunk bottoms (43–51%).

The maximum values of the integral moisture content of the soil and vegetation cover (63–69%) were recorded at points confined to the forested or shaded trunk bottoms or to the "cold" gentle slopes under shrouded steppe meadows. Natural complexes that are subject to anthropogenic impact are able to retain less moisture in comparison with reserved analogs (47–52% and 58–63%, respectively). The minimum values of integral humidity (18–27%) are determined on steep, almost talus southern slopes with underdeveloped vegetation. The low integral humidity of the sparse and steppe LC of the southern slopes and flat terraces is compounded by a small projective cover of the grass stand (15–40%) or a low crown density not exceeding 0.3. An important circumstance is a large proportion of cereals (e.g., aegilops) with dried aerial parts in the vegetation cover. Shrub vegetation (hold-tree, pear-leaved pear, which has a little foliage) or fluffy oak prevails on light-forested points with minimal integral humidity.

Validation of NDWI Values. The integral indicator of soil moisture is described by NDWI values calculated on June 15, 2016, with a determination coefficient of $R^2 = 0.72$. The dependence is violated due to samples taken in the steppe tracts of ridges and steep northern slopes, where the distance information is clearly distorted due to the relief and chiaroscuro (these points are marked in Figure 3 with an "X"). If we consider this relationship separately for different types of landscape cover, then the accuracy of the description increases to $R^2 = 0.90–0.91$. The dependence of field humidity and ~~humidity~~ NDWI on the southern slopes occupied by steppe and shrub-steppe vegetation is noticeably different, where NDWI is more sensitive to changes in field humidity (shown in square 3 by square symbols) on other points forests and steppes of flat apical surfaces and gentle northern slopes, where NDWI grows more slowly (shown in Figure 3 by round icons).

The high reliability of the description of the integral moisture content of the soil and vegetation cover with ~~the moisture~~ NDWI calculated for the sampling period made it possible to switch from the dynamics of the field moisture content to the spatial picture of the dynamics of NDWI values.

Seasonal Moisture Dynamics. The rate of moisture loss by soil-vegetation cover is expressed in terms of the difference in the NDWI (NDWI-Dif) calculated for the conditions of maximum saturation of the soil and vegetation with moisture and on the date of interest. The study examined the change in soil moisture from May 14 to August 27, 2016. Many factors were checked to construct an accurate statistical model; the NDWI-Dif showed the highest correlation: the NDVI on August 27, 2016 (relative indicator of the amount of photosynthetically active phytomass), the amount of potential incoming solar radiation (PPPS, which determines the evaporation rate), and the NDWI for May 14, 2016 (which characterizes the moisture accumulated in the soil–plant cover to the beginning of the dry period). They are included in the statistical model describing the seasonal difference in NDWI. Interestingly, the morphometric characteristics of the relief did not show a relationship with the rate of moisture loss. The relief has an indirect effect through the PPPP index and also "turns on" in the bottoms of erosion forms.

The most powerful factor determining the magnitude of seasonal moisture loss is the amount of photosynthetically active phytomass, which is described by NDVI. The determination coefficient for the association of NDVI for August 27 with NDWI-Dif is $R^2 = 0.63$. LC with a large proportion of bare soils and intensive development of slope processes has a low ability to retain moisture and low NDVI both in early summer and in autumn but a significant difference in NDWI, which is obviously achieved due to soil drying. Dry steppe and steppe LC has a higher NDVI at the

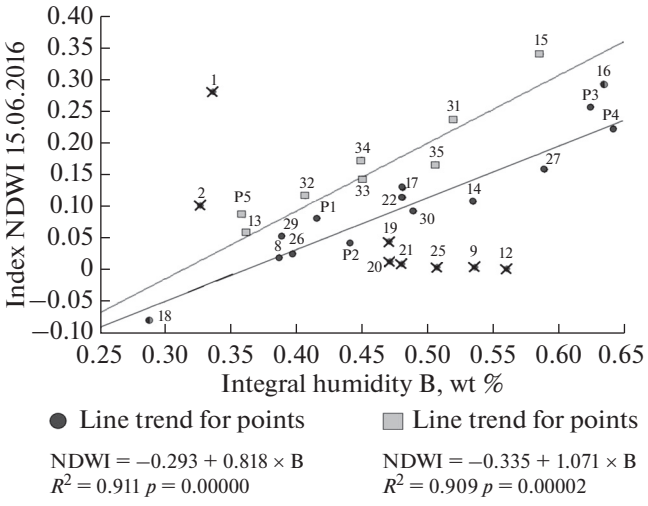

Fig. 3. Relationship between integral field moisture (M) and NDWI.

beginning of summer, but both soil and grass vegetation are very dry by August (NDVI decreases, followed by NDWI); therefore, they also have high NDWI-Dif. Light forests have a higher NDVI and ability to retain moisture in the vegetation cover, while the decrease in NDVI per season is lower; therefore, the total moisture loss is also reduced. Finally, forests have maximum values and minimal NDVI differences during the dry period, and the moisture reserves in their foliage and grass cover experience a minimal drop. It is worth noting that the sets of points overlap quite strongly: for example, ash forests with a high holding tree have approximately the same NDWI-Dif value as oak woodlands with a crown density of about 0.3 and a fraction of bare soil of about 0.2. The reason for this in the first case is the strong drying of the leaves of ash and hold-tree and its partial decline; in the second, it is the rapid drying of the bare soil.

For spatial calculations, the Multiple Regression Analysis module was used ~~in the SAGA program~~, which receives raster data of variables (factors) and models each pixel of the dependent variable. Each type of landscape cover is analyzed separately, and the territories of settlements are excluded. The results of this analysis are presented in Table 1. The best accuracy of the model is recorded for vineyards ($R^2 = 0.94$), typical steppes ($R^2 = 0.83$), and light forests ($R^2 = 0.89$). Slightly less acceptable modeling results are observed for dry and petrophytic steppes with steep "badlands" slopes ($R^2 = 0.76$). The model for forest LC is the least clear .

The leading role of vegetation is also manifested in the transition from field research points to pixels of distance images. NDVI describes 39% (in forests) to 75% (in typical steppes) variations in the seasonal difference of NDWI. In dry steppes with a small phytomass ~~of vegetation~~, the amount of incoming solar radi-

Table 1. Results of multiple regression analysis of the intensity of moisture loss in the soil-vegetation cover for different types of landscape cover

Type of landscape cover	R^2	Standard error	Regression coefficient for factors		
			NDVI for 08.27	PPSR	NDWI for May 14
Dry and petrophytic steppes, badlands	0.76	0.054	0.114	0.212	0.002
Typical steppes	0.83	0.029	0.547	0.075	0.102
Sparse woodlands	0.89	0.028	–0.660	0.302	0.757
Woods	0.67	0.033	–0.370	0.337	0.057
Vineyards	0.94	0.005	–0.811	0.174	1.596

ation plays a decisive role, heating the soil and promoting the evaporation ~~of moisture from it~~. In typical steppes, the role of vegetation increases. The grass cover~~, even continuous cover,~~ loses much moisture during the dry period (Morozova and Vronsky, 1989); therefore, an increase in the phytomass in the steppe LC leads to an increase in NDWI-Dif in them. This explains why most of the natural fires in the east of the Crimean mountains are in the steppe and can be used to identify fire-hazardous areas. In light forests, the role of the vegetation cover is still increasing, but the sign of its influence is changing: the more active phytomass is, the less active is NDWI-dif. A significant value is the initial moisture supply. In the forests that hold moisture best, the main factors are the phytomass ~~of vegetation~~ (NDVI) and the amount of incoming solar radiation.

CONCLUSIONS

1. Modeling of the moisture content of the LC based on the NDWI shows a higher reliability when the landscape structure of the territory is taken into account. The study revealed a high significance of the contribution of not only plant formations but also the exposure and steepness of the slopes. With the landscape approach, the modeling accuracy for individual types of tracts reaches $R^2 = 0.90–0.91$.

2. The redistribution of moisture over the relief does not play a significant role in the formation of humidification conditions in the semiarid low mountains of the Crimean mountains. Precipitation either evaporates quickly or is quickly carried out by the erosion network; it does not linger on either concave or gentle slopes. The exception is the bottoms of large erosion forms composed of loose deposits that can retain moisture.

3. Vegetation is a factor stabilizing the dynamics of moisture in the soil and vegetation cover. The most stable is forest LC. The maximum moisture loss during the growing season is observed in the steppe landscapes.

4. In the prediction of the dynamics of moisture in the soil-vegetation cover, the statistical regression model includes the vegetation index, the amount of potential incoming solar radiation, and the initial (spring) moisture reserve. The best predictions are for the LC of vineyards and woodlands, while the predictions for forests are the worst.

5. Distance information is distorted on the steep northern slopes, which constitutes a limitation of this method.

REFERENCES

Böhner, J. and Selige, T., Spatial prediction of soil attributes using terrain analysis and climate regionalization, *Göttinger Geogr. Abh.*, 2006, vol. 115, pp. 13–27.

Carlson, T., An overview of the "triangle method" for estimating surface evapotranspiration and soil moisture from satellite imagery, *Sensors*, 2007, vol. 7, pp. 1612–1629.

Ceccato, P., Gobron, N., Flasse, S., Pinty, B., and Tarantola, S., Designing a spectral index to estimate vegetation water content from remote sensing data: Part 1. Theoretical approach, *Remote Sens. Environ.*, 2002, vol. 82, pp. 188–197.

Dobson, M.C. and Ulaby, F.T., Active microwave soil moisture research, *IEEE Trans. Geosci. Remote Sens.*, 1985, vol. GE-24, no. 1, pp. 23–36.

Escorihuela, M.J. and Quintana-Seguí, P., Comparison of remote sensing and simulated soil moisture datasets in Mediterranean landscapes, *Remote Sens. Environ.*, 2016, vol. 180, pp. 99–114.

Gao, B.-C., NDWI—A normalized difference water index for remote sensing of vegetation liquid water from space, *Remote Sens. Environ.*, 1996, vol. 58, no. 3, pp. 257–266.

Ghulam, A., Li, Z.-L., Qin, Q., Yimit, H., and Wange, J., Estimating crop water stress with ETM+NIR and SWIR data, *Agric. For. Meteorol.*, 2008, vol. 148, pp. 1679–1695.

Gillon, D., Dauriac, F., Deshayes, M., Valette, J.C., and Moro, C., Estimation of foliage moisture content using near infrared reflectance spectroscopy, *Agric. For. Meteorol.*, 2004, vol. 124, pp. 51–62.

Gorbunov, R.V., Zuev, A.V., and Smirnov, V.O., *Water-balance studies in Karadag landscape-ecological stationer, in 100 let Karadagskoi nauchnoi stantsii im. T.I. Vyazemskogo* (Collection of Scientific Research Works Dedicated to the 100 Anniversary of Karadag Scientific

Station Named after T.I. Vyazemskii), Simferopol: N. Orianda, 2015, pp. 734–747.

Maki, M., Ishiahrab, M., and Tamura, M., Estimation of leaf water status to monitor the risk of forest fires by using remotely sensed data, *Remote Sens. Environ.*, 2004, vol. 90, pp. 441–450.

Moran, M.S., Clarke, T.R., Inoue, Y., and Vidal, A., Estimating crop water deficit using the relation between surface-air temperature and spectral vegetation index, *Remote Sens. Environ.*, 1994, vol. 49, pp. 246–263.

Morozova, A.L. and Vronskii, A.A., *Priroda Karadaga* (Karadag Nature), Kiev: Naukova Dumka, 1989.

Nijland, W., Coops, N.C., Macdonald, S.E., Nielsen, S.E., Bater, C.W., White, B., Ogilvie, J., and Stadt, J., Remote sensing proxies of productivity and moisture predict forest stand type and recovery rate following experimental harvest, *For. Ecol. Manage.*, 2015, vol. 357, pp. 239–247.

Peuelas, J., Filella, I., Biel, C., Serrano, L., and Sav, R., The reflectance at the 950-970 nm region as an indicator of plant water status, *Int. J. Remote Sens.*, 1993, vol. 14, no. 10, pp. 1887–1905.

Sadeghi, M., Babaeian, E., Tuller, M., and Jones, S.B., The optical trapezoid model: A novel approach to remote sensing of soil moisture applied to Sentinel-2 and Landsat-8 observations, *Remote Sens. Environ.*, 2017, vol. 198, pp. 52–68.

Seneviratne, S.I., Corti, T., Davin, E.L., Hirschi, M., Jaeger, E.B., Lehner, I., Orlowsky, B., and Teuling, A.J., Investigating soil moisture–climate interactions in a changing climate: a review, *Earth-Sci. Rev.*, 2010, vol. 99, nos. 3–4, pp. 125–161.

Shvetsov, E.G., Ruzhichka, Z., and Mironov, V.L., Applicability of SMOS satellite data for evaluation of wild fire danger in Krasnoyarsk krai, *Vestn. Sib. Gos. Agrar. Univ.*, 2013, no. 2 (48), pp. 110–115.

Sysuev, V.V., *Fiziko-matematicheskie osnovy landshaftovedeniya* (Physical-Mathematical Basis of Landscape Science), Moscow: Mosk. Gos. Univ., 2003.

Transformatsiya landshaftno-ekologicheskikh protsessov v Krymu v XX veke–nachale XXI veka (Transformation of Landscape-Ecological Processes in Crimea in 20th Century–Beginning 21st Century), Simferopol: Dolya, 2010.

Yebra, M., Dennison, P.E., Chuvieco, E., Riaño, D., Zylstra, P., Hunt, E.R., Jr., Danson, F.M., Qi, Y., and Jurdao, S., A global review of remote sensing of live fuel moisture content for fire danger assessment: moving towards operational products, *Remote Sens. Environ.*, 2013, vol. 136, pp. 455–468.

Wigneron, J.-P., Chanzy, A., Calvet, J.-C., and Bruguier, N., A simple algorithm to retrieve soil moisture and vegetation biomass using passive microwave measurements over crop fields, *Remote Sens. Environ.*, 1995, vol. 51, no. 3, pp. 331–341.

SPELL: 1. OK